EPRG-PRCI-APGA
23rd Joint Technical Meeting
Edinburgh, Scotland
6–10 June 2022

PAPER TITLE: NUMERICAL INVESTIGATION OF RISKS ASSOCIATED WITH DECOMPRESSION AND ATMOSPHERIC EXPANSION OF HYDROGEN PAPER NUMBER: 12

Dr Xiong Liu, Dr Guillaume Michal*, Prof Cheng Lu, Dr Ajit Godbole
MMMBE School, University of Wollongong, NSW Australia

Dr. Kamal K. Botros
NOVA Chemicals Corporation, Canada

* presenting author

ABSTRACT

The Future Fuels CRC engaged NOVA Chemicals to conduct a decompression tube test program at the TC Energy's Gas Dynamic Test Facility in Didsbury, Canada aimed at assessing the accuracy of the decompression model and equations of state for natural gas and hydrogen blends. The first test was conducted on pure hydrogen from initial pressure of approx. 17 $MPa_{(a)}$. The decompression wave speed was successfully measured. Good agreement between model and experiment was observed.

The test indicated relatively higher noise and overpressure levels in excess of what was typically observed at the site from numerous tests with natural gas and dense-phase CO_2 mixtures. Ignition was qualitatively witnessed 'immediately' after the rupture disc was triggered. Although insufficient data is available to conclude if this qualifies as spontaneous ignition of hydrogen, published studies on the topic would suggest that this could be the case.

Risks from atmospheric overpressure waves, noise levels and possible ignitions influence the safety of a range of operations such as pipe rupture, venting, blowdown, etc. A better understanding of the risks associated with high-pressure hydrogen releases and their atmospheric expansion is warranted.

Following a summary of the outcomes of the first decompression test, this paper reports on the results of a computational fluid dynamics study aimed at replicating the environment of the test conditions conducted on pure hydrogen. The primary goal of the study was to compare the aforementioned risks from the decompression of methane and pure hydrogen.

The Peng-Robinson EOS was employed in the analysis via user-defined functions to calculate the thermodynamics properties of H_2/air or CH_4/air mixtures in the atmosphere at runtime. The strength of the overpressure, noise levels and temperature variations were analysed. Published tables of likelihood of damage to structure and human body formed the basis to weight the relative risks between the two mixtures. Potential methods to mitigate the levels of impact during a controlled release are discussed.

DISCLAIMER

1. INTRODUCTION

Climate science recommended that limiting global warming to below 2 °C requires that Carbon Dioxide (CO_2) emissions decline by around 25% by 2030, compared to 2010 levels, and reach net zero emission by around 2070 [1]. To achieve the warming target, an energy transition is needed to 'decarbonise' our economy. Among a number of transformational technologies, the application of renewable Hydrogen (H_2) has been recommended as an important part of CO_2 emission mitigation efforts in the coming decades.

A wide application of H_2 requires efficient and cost-effective transportation. If there is sufficiently large and sustained demand, transmission pipelines are likely to be the most appropriate long-term choice for H_2 distribution [2]. Fracture propagation is a significant issue for transmission pipelines. A plan to control running ductile fracture which involves the accurate understanding of the decompression characteristics of H_2 must be provided to facilitate its transport [3].

Decompression of gases can be studied through experimental or numerical methods. Experimental methods such as decompression tube test or full-scale burst test have been widely used for denser gases like Natural Gas (NG) or CO_2 [4], [5], [6], [7]. Limited experimental programs have been conducted with NG+H_2 blends [8].

Unlike NG or CO_2, a release of high-pressure H_2 features much higher release velocity. The speed of sound of pure H_2 is in the order of 1,000 m/s; several times the magnitude of the speed of sound of NG or CO_2. At equal initial pressure and release orifice area, the peak release rate of NG is about 3.4 times that of H_2. However, as the density of NG under ambient pressure is about 7.3 times that of H_2, the released volume of H_2 will be over 2 times of that of the NG under ambient pressure. This implies that the released H_2 will undergo much greater volumetric expansion than NG.

The higher release velocity and greater volumetric expansion of H_2 may lead to stronger pressure field in the atmosphere, and higher instantaneous temperatures across the shock developing in the first instants of the atmospheric expansion. These may cause risks to nearby personnel or facilities, such as excessive overpressure, noise level, or spontaneous ignition.

As part of its research project "RP3.2-02", the Future Fuels CRC engaged NOVA Chemicals to conduct a decompression tube test program aimed at assessing the accuracy of the isentropic decompression model and several equations of state. The first test, conducted at TC Energy's Gas Dynamics Test Facility in Didsbury, Alberta, Canada, investigated the rapid decompression of pure H_2 from an initial pressure of approx. 17 $MPa_{(a)}$. This test indicated noise levels in excess of what was typically witnessed at the site with NG and CO_2 mixtures. Ignition was qualitatively witnessed 'immediately' after the onset of the rupture disc in an external ambient environment free of ignition source.

Risks from overpressure wave, noise level, vibration and ignition influence the risk assessment of H_2 pipelines following an accidental release and the safety of controlled releases such as venting, blowdowns. Thus, a better understanding of the risks associated with high-pressure H_2 releases and their atmospheric expansion is warranted. Capitalising on the industry knowledge with methane, it is appropriate to consider the characteristics of H_2 release in absolute terms and relative to methane.

In this work, a summary of the outcomes of the H_2 decompression test is first reported. It is followed by a Computational Fluid Dynamics (CFD) study aimed at replicating the conditions of the shock tube test on pure H2 conducted at the TCE site. The primary goal of the study is to compare the aforementioned risks from the decompression of methane and pure hydrogen. Potential methods to mitigate the levels of impact during a controlled release are discussed.

2. HYDROGEN DECOMPRESSION TUBE TEST

The Battelle Two-Curve Method (BTCM) informs that the minimum required toughness to arrest a running ductile fracture depends on the velocity of the fracture and the decompression wave velocity of the gas mixture [3], [4]. A mixture with a faster decompression wave speed (W) leads to a lower toughness requirement. At equal available toughness, a faster decompression is synonymous with a shorter distance required to arrest the fracture [9].

A recent study indicated the decompression characteristic of lean gas and hydrogen blends containing up to 8% of hydrogen can be well predicted [8]. Other than that study, experimental decompression wave speed from mixtures with significant amount of hydrogen are either very limited or unpublished. Owing to the importance of accurate predictions of the decompression wave speed for hydrogen blends, the RP3.2-02 Future Fuels CRC project is investigating the performance of a range of equations of states at higher hydrogen content and richer gas mixtures.

The project is supported by an experimental decompression tube test campaign covering nine distinct test conditions (pressure, temperature, composition), all in duplicates. The mixtures span a range of rich gases made of methane, ethane, and hydrogen. Test pressures range from 10.5 to 17 MPa(a). The first test was conducted in February 2022 using pure hydrogen pressurised at 16.6 MPa at a temperature of -1.5 °C.

The following section provides background relevant to the decompression wave speed model and its links to thermodynamic properties of a mixture. It is followed by a brief description of the decompression tube test experiment and the characteristics of the tube available at the test. The outcomes of the test with pure hydrogen are then discussed.

2.1. Decompression Wave Speed

Equations 1 to 3 present the numerical scheme used to evaluate the decompression wave speed within the framework of the unidimensional inviscid and isentropic decompression model used in the BTCM. The depressurisation takes place from the operating pressure P_o down to the choke pressure P_c. In Eq. 1, $\Delta P < 0$ is the depressurisation pressure step. ρ and C are the density and speed of sound of the mixture at the pressure P along the isentropic decompression path s. U is the outflow velocity. W is the decompression wave speed and, by definition of the choke condition, $W(P_c) = 0$.

$$\Delta U = -\frac{\Delta P}{\rho . C}\bigg|_s \tag{1}$$

$$U(P) = \sum \Delta U \tag{2}$$

$$W(P) = C - U \geq 0 \tag{3}$$

The thermodynamics properties ρ and C at each pressure are calculated using an equation of state using (P, s) as state variables. The speed of sound C is the partial derivative of pressure with respect to the density at constant entropy:

$$C(P, s) = \sqrt{\frac{\partial P}{\partial \rho(P)}\bigg|_s} \tag{4}$$

The speed of sound of hydrogen is in the order of 1000 m/s. That of methane is less than half that of hydrogen at the same initial P and T. Close to P_o, the wave speed in H_2 is in the order of twice that of methane. Close to P_c, both decompression wave speeds go to zero. The choke pressure of each

decompression process is normally different. Whether the decompression wave speed of a hydrogen blend remains faster than that of methane depends on C (Eq. 4); but it also depends on the evolution of the product $\rho.C$ along the isentropic decompression path (Eq. 1).

Numerical studies can be conducted to predict the decompression wave speed for a range of mixtures using numerical decompression tools [4] [10]. The accuracy of modern equations of states (EOS) has been studied and validated for lean (dry) and rich (wet) natural gas mixtures [6], [5] and a range of anthropogenic CO_2 mixtures [7].

Over the years, the GERG 2008 EOS has proved to be a reliable and performant computing library [11]. Only limited studies focused on its performance and that of other EOS for mixtures with a hydrogen fraction above 10% mole. Such performance assessments are supported by decompression tube tests.

2.2. Decompression Tube Test

A decompression tube, also called a shock tube, a rupture tube or an expansion tube, is a cylindrical device made of an insulated pipe section, long relative to its internal diameter. The ratio of the tube length to its inner diameter is typically in the range of 500 – 1000 with an inner diameter in the order of 50 to 150 mm. The geometry of the tube lends itself to the one-dimensional approximation of the model. See Figure 1 for an illustration.

The "back" of the tube, shown on the right side of the figure, is fully closed. The front end, on the left end side of the figure, is fitted with a rupture disk to close the tube during the pressurisation and circulation phase. The rupture disk is a component able to create a full-bore opening very rapidly by mean of a bead of explosive or using a specific score on its surface. The scoring is precision-made to initiate a rapid full-bore opening at a targeted pressure and temperature, see Figure 2.

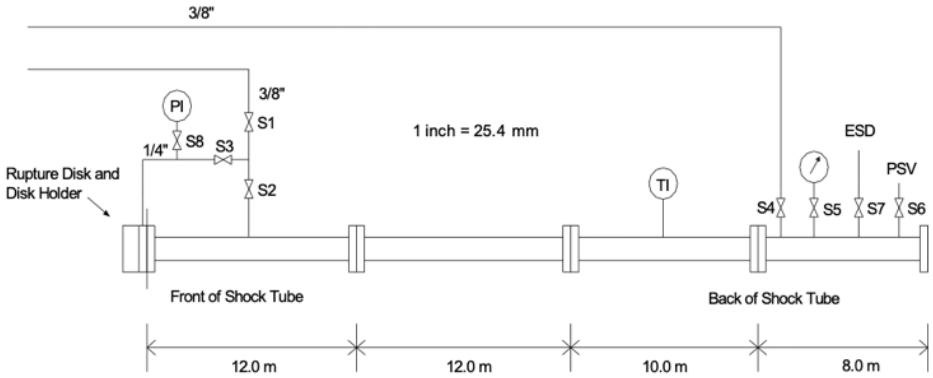

Figure 1 Schematic of the decompression tube available at TCE, from [12].

Figure 2 (left) X-scored and (right) O-scored rupture disks, from [12].

A circulation loop with a heater and chiller is connected to the tube. The loop is isolated during the experiment by closing an upstream and a downstream valve. The loop is used during the setup phase to carry out several operations. First the system is purged, using nitrogen for example, then flushed. The components of the mixture are progressively added while monitoring the composition. The

pressure is progressively increased up to a pressure below that of the rupture disk's failure pressure. The circulation continues to mix the components until a homogenous mixture and a target temperature is achieved. The loop is then isolated from the tube and the pressure is increased until rupture of the disc.

The tube is fitted along its length with calibrated high resolution, low latency, pressure and temperature transducers. The pressure signals are sampled at a rate typically between 1 kHz and 100 kHz depending on the setup.

A transient decompression process initiates upon rupture of the disc. The decompression waves travel upstream, towards the closed end of the tube. The high velocity – high pressure waves precede the lower velocity–lower pressure waves. Each pressure transducer observes a progressive but rapid drop in pressure as function of time. The measured pressure-time profile depends on the velocity of each decompression wave. It is characteristic of the mixture behaviour along its isentropic decompression path. Transducers further away from the rupture disc present lower decompression rates than those close to it. In theory the signals are homothetic relative to the location of the rupture disc.

Given enough time the first decompression wave will reach the closed end of the tube. The wave will be reflected. It will then travel back in the downstream direction, towards the open end of the tube. The calculation of the wave speed between two transducers is valid as long as the first reflected wave does not reach the farthest transducer used in the calculation.

The longer the tube, the lower the pressure point at which the decompression wave speed can reliably be measured: more time is given for the slowest waves to travel between the first two transducers before the reflected wave arrives. The minimum wave speed that can be measured is above the choke pressure. By definition, the wave at choke pressure does not travel upstream ($W = 0$), thus no valid data exist between consecutive transducers at that pressure.

A recent description of the test setup used in this study is detailed in [8]. A brief overview is provided here. The TC Energy's Gas Dynamic Test Facility has a permanent 42 m long decompression tube. The tube is made of four NPS 2 stainless steel spools with a wall thickness of 11.1 mm and an inner diameter of 38.1 mm. The inner surface of the tube is honed to 0.635 μm to minimise frictional effects. 14 pressure transducers are mounted along the tube, of which 11 are distributed within the first spool from the location of the rupture disc. The pressure-time trace at each transducer typically records at 51.2 kHz, equivalent to a data resolution of 19.53 microseconds, to capture a maximum of 16,384 data points within a timeframe of 320 ms.

2.3. First Experimental Decompression Of Pure Hydrogen

The test was conducted on the 3rd February 2022. Hydrogen class 5.0, ultra-high purity (99.999%) was used to fill the tube. Pressure and temperature at the instant of failure of the rupture disc was 16.62 MPa(a) and -1.5 °C.

Data was successfully recorded over a timeframe of 320 ms from the transducers used in the test, namely PT1, PT1A, PT1B and PT2 to PT11. Figure 3 presents the raw pressure-time traces from the transducers. The quality of the acquisition is excellent with a very low noise to signal ratio. It is noted that transducer PT2 and, to a lesser extent PT3 as well as PT8, recorded a higher level of periodic noise in the order of 3 kHz.

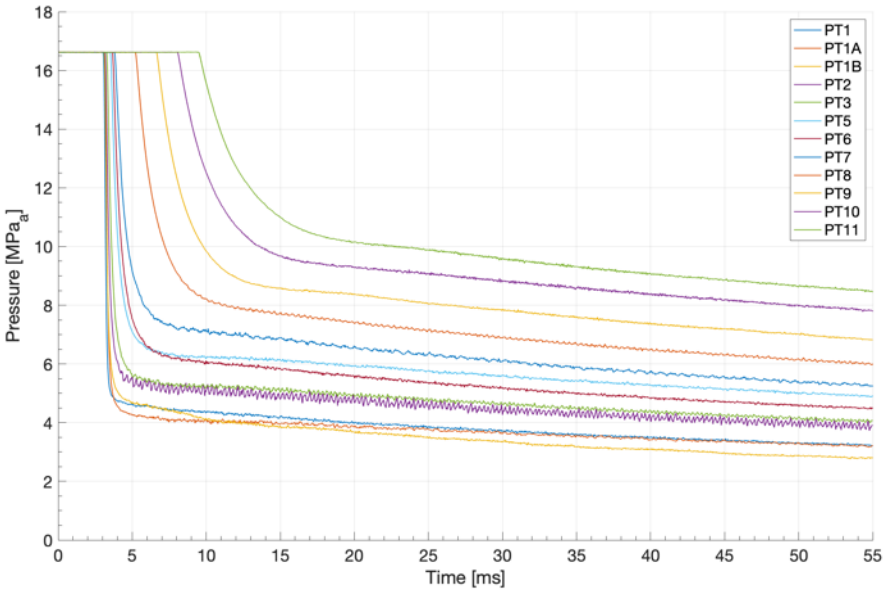

Figure 3 Pressure - time traces from the pure hydrogen decompression test.

The experimental decompression wave speed was calculated in a traditional manner by following the isobar at different pressure points across the pressure-time traces. The velocity of a wave at a given pressure is obtained by identifying the timelapse between the arrival of that wave from consecutive transducers. The wave speed is the ratio of the distance separating the two transducers by that timelapse.

Figure 4 present the experimental data along with the prediction using the GERG 2008 EOS from the decompression model implemented in EPDECOM [10]. The measured decompression wave speed starts at 1402 m/s at the initial pressure. The predicted initial velocity is 1410 m/s, less than 0.6% above the experiment. The initial velocity is difficult to quantify with a high degree of accuracy. Small variations from the initial pressure can be misjudged as the arrival of the first wave. The almost horizontal trend observed at the beginning of the experimental curve is an artefact of the data processing.

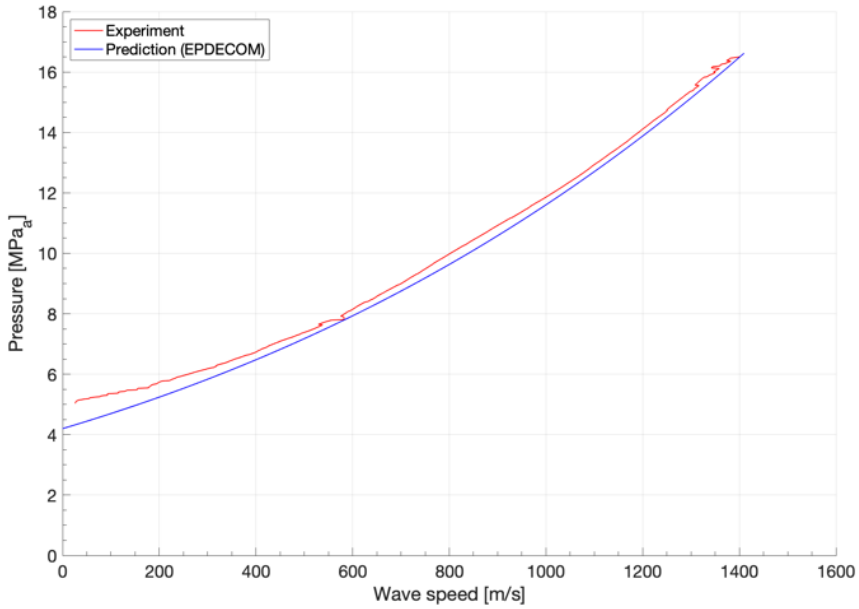

Figure 4 Measured and predicted decompression wave speed for pure hydrogen at 16.62 MPa(a) and -1.5 °C.

Other than the initial decompression wave speed, the remaining experimental characteristic is above the prediction. That is, waves travelled slightly slower than predicted. The difference is minor at velocities above 600 m/s. Below that velocity, the two curves diverge more noticeably. In the context of the BTCM, this indicates a degree of non-conservatism of the prediction. The minimum required toughness would be slightly underestimated.

In [13], Lu et. al investigated the effects of friction on the decompression wave speed of natural gas mixtures. It was shown that frictional effects tend to decrease the velocity of the waves towards the tail of the decompression curve. The effect is more noticeable for pipes with a diameter below 250 mm. While the diverging trend between the experiment and the prediction is expected, further analysis will be required to evaluate its severity relative to previous tests.

The impact of frictional effects can be of particular importance. The interaction between the decompression wave speed curve and the fracture velocity typically occurs at velocities well below 600 m/s. Although this depends on the pipe geometry and its properties, theoretical interactions below 300 m/s would be considered typical. The prediction deviates by 0.5 to 0.8 MPa from 300 m/s down to 30 m/s, or a deviation in pressure between 8 and 16%.

Further work is required to evaluate if the observed effect is solely the result of frictional effects and to consider why it appears to be more prominent in H_2 than would be expected from the decompression of natural gas. It is postulated that the larger flow velocity inside the tube may contribute to this outcome. In [13], the authors concluded that frictional effects are not an issue for natural gas transport in pipes above 250 mm in diameter. This threshold may need to be revised for pure hydrogen gas transport or blends containing primarily hydrogen.

Overall, the predictions from the isentropic inviscid decompression model are considered good at high velocities. Further work is required to understand the role of friction and other factors in the observations made at low decompression wave velocities.

2.4. Other Experimental Observations

Other than the possible increase in frictional effects, three other aspects of the tests highlighted the differences in decompression behaviour between natural gas and hydrogen.

The shock tube is located on an experimental site with numerous buildings and piping infrastructure. One building is located 4.2 m downstream from the exit of the tube, with one of its windows facing the tube. Concrete blocks are placed between the building and the exit of the tube. Other buildings are located outside a 30 m radius exclusion zone. This configuration has remained essentially unchanged over the past 150 tests conducted with various natural gas and CO_2 mixtures. The test personnel is experienced with the established test and OH&S procedures. Noise and debris displaced by the outflow are expected.

A dummy test with natural gas was conducted prior to the first test to confirm readiness of the setup. The hydrogen test followed. The release of hydrogen from the instant of rupture of the disc was immediately followed by a loud noise akin to a detonation. This form of noise is typical of the sudden release of a highly pressurised gas. It is an anticipated consequence of the release. However, the level of noise generated was considered louder than experienced from tests with either natural gas or carbon dioxide from the same initial P and T.

The level of noise is associated with the overpressure waves that are generated during the expansion of the gas in the atmosphere. The concrete blocks placed between the tube and the downstream building limit the propagation of the overpressure waves towards the building. Nonetheless, the front

window located behind the blocks experienced some damage; a situation which had not been witnessed in previous tests. This observation corroborates the perception that the noise levels were higher than usual.

The outflow of hydrogen constrained between the exit of the tube and the concrete blocks ignited "immediately" according to witnesses. The limited amount of gas in the tube and the short duration of the test led to a brief but bright combustion. Evidence of elevated heat was observed in the proximity of the tube's exit. Ignition has not been witnessed in past tests. The area was free from ignition sources in accordance with OH&S requirements. Auto-ignition of hydrogen may be the mechanism supporting this outcome.

These observations indicates that some of the test's outcomes went beyond expectations. The decompression characteristics of hydrogen led to increased outflow velocities, increased noise level, increased overpressure waves and increased susceptibility to ignition relative to previous experience with other flammable gas conducted at the site.

In the following sections, a range of CFD simulations are presented. The intent of these simulations is to highlight the differences between hydrogen and methane, and to explain the mechanisms supporting the experimental observations relevant to overpressure, noise and ignition risks during the expansion of hydrogen in the atmosphere.

3. CFD MODEL FOR ATMOSPHERIC EXPANSION STUDIES

A CFD study aimed at replicating the environment of the test program conducted at the site was carried out to evaluate the risks associated with high-pressure H_2 releases and their atmospheric expansion. The computational domain used in the model was determined according to the geometry of the test tube.

The propagation of pressure waves for the purpose of capturing overpressures and noise levels requires a fine meshing of the domain. This translates to significant computational resources and lengthy simulations in the three-dimensional space. A two-dimensional axisymmetric model is adequate to capture the principal metrics of interest. It permits to conduct parametric studies in a shorter timeframe from which a first set of conclusions can be drawn. The exponential decay associated with the propagation of overpressure waves and noise levels is important to capture. At equal computational cost, a two-dimensional model axisymmetric domain can be extended to larger distances to account for a wider range of severity levels.

The axisymmetric model has its limitations. It cannot describe reflections of pressure waves occurring against the ground and surrounding infrastructures. Although not reported here, three-dimensional simulations specific to the test site were also initiated and are continuing. The purpose of these simulations is two-fold. First, they provide a mean of comparison with the axisymmetric model to study the impact of reflections with ground and infrastructures. Second, they provide detailed and specific information relevant to the test site.

Figure 5 shows a schematic of the domain. It is delimited by a pressure-based outlet boundary condition with constant ambient pressure and temperature located along a 50 m radius, centered relative to the shock tube's exit plane. A no-slip wall boundary condition is assigned along the inner wall of the tube and its closed end. The internal volume of the tube contains pure H_2 or pure CH_4 at initial pressure and temperature condition. The ambient environment is made of a mixture representative of air (79% N_2 + 21% O_2) at atmospheric pressure.

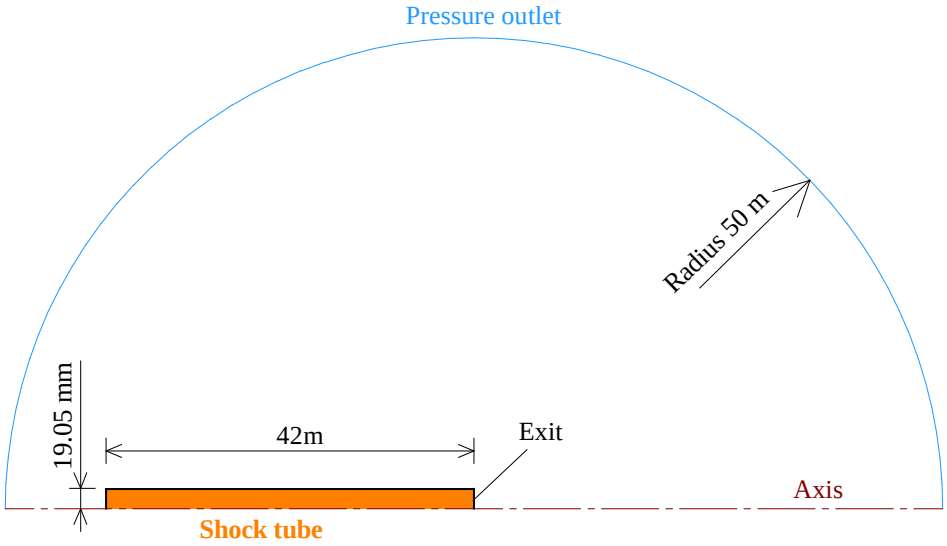

Figure 5: Computational domain (not to scale)

ANSYS Fluent is employed for the simulations. The Peng-Robinson EOS [14] is implemented via user-defined functions to estimate the thermodynamics properties of H_2/air or CH_4/air mixtures at runtime. The realisable *k*-ε model is chosen for turbulence modelling. The density-based solver is used for the solution.

During the simulation, pressures are monitored at 4.2 m, 5m, 10 m, and 15 m downstream from the exit plane of the tube. The downstream monitoring point at 4.2 m is indicative of the location of the nearby building at the site. Flow variables such as temperature, pressure, velocity, and concentration are also monitored in the near field of the jet expansion.

4. CFD SIMULATION RESULTS

The initial pressure and temperature in the tube are close to that reported in the hydrogen experiment, at 17 MPa and 0 °C respectively. The atmospheric expansion of pure H_2 and then pure CH_4 was studied over a timeframe of 80 ms from the instant of release. The latter is defined as the instant of failure of the rupture disc.

4.1. Overpressure

Following the rupture of the disc, a pressure wave is generated in the atmosphere due to the expansion of the compressed gas. The pressure wave travels at speed higher than the speed of sound in the atmosphere depending on the overpressure. Overpressure levels are linked to a range of damages to infrastructures and injuries to animals and humans. Sudden changes in pressure can affect pressure-sensitive organs such as ears and lungs. Much knowledge is available in the literature on the topic, typically originating from studies relevant to blasting and explosives. Table 1 relates overpressure levels to the structural and physiological effects produced [15].

Figure 6 shows the predicted overpressures produced by H_2 expansion at different downstream locations. The maximum overpressure at a given location occurs at the beginning of the passing wave. The closer the location from the point of release, the higher is the initial rate of increase in overpressure strength, and the higher is the maximum. After a short period of decline, the pressure increases again and reaches a second peak. The overpressure drops sharply afterwards; a precursor to the propagation of the incoming rarefaction wave. A strong negative pressure develops close to the release point. A more progressive transition back to atmospheric pressure follows. Spurious variations continue over a longer, albeit still short, timeframe.

Overpressure (psi_g)	Expected damage
0.15	Typical pressure for glass failure.
0.40	Limited minor structural damage.
0.70	Minor damage to house structures.
1.0	Partial demolition of houses; made uninhabitable.
2.0	Partial collapse of walls and roofs of houses.
2.0-3.0	Non-reinforced concrete or cinder block walls shattered.
2.4-12.2	Range for 1-90% eardrum rupture among exposed populations.
3.0	Steel frame buildings distorted and pulled away from foundation.
5.0	Wooden utility poles snapped.
5.0-7.0	Nearly complete destruction of houses.
7.0	Loaded train cars overturned.
9.0	Loaded train box cars demolished.
10.0	Probable total building destruction.

Table 1 Level of damage expected at specific overpressure values [15]

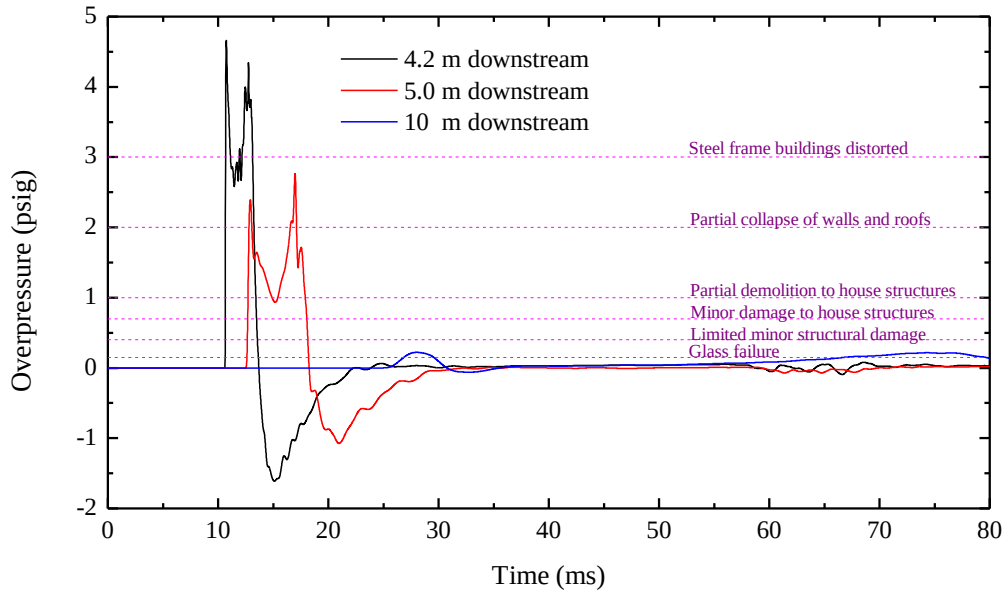

Figure 6: Overpressure histories predicted at different downstream locations (H_2, 17 MPa)

The overpressure at 4.2 and 5 m downstream show a similar pattern. However, the latter presents a second peak exceeding its first peak. The initial overpressure phase decreases in magnitude by about half. Its timeframe extends because the leading and trailing fronts of the overpressure wave are propagating at different velocities. The density of energy decreases over time as the overpressure wave spreads in space. The front of the wave propagates at about 390 m/s, slightly higher than the speed of sound in air at ambient pressure.

Figure 6 also reports the levels of damage summarised in Table 1. The overpressure produced by the expansion of pure H_2 initially compressed at 17 MPa can cause substantial damage within the first 5 m. At 4.2 m the overpressure exceeds the threshold leading to possible distortion of buildings with a steel frame. Building's foundations can be impacted. It is noted that the level of damage will also depend on the surface area over which the building experiences a given overpressure threshold. This depends on the diameter at the point of release. Figure 6 indicates that the magnitude of the overpressure decreases by an order of magnitude from 5 m to 10 m.

Figure 7 shows the maximum overpressure experienced along the jet axis. The maximum overpressure reduces exponentially along the jet axis. At 5 m downstream, its peak value reduces to 2.8 psi, from 4.7 psi at 4.2 m. At 10 m, the maximum overpressure reduces to only 0.22 psi. It is noted that the latter is still sufficient to cause glass components to fail. At about 12 m downstream from the exit, the overpressure will reduce to below 0.15 psi.

Figure 8 shows the overpressure over the jet's cross section taken 4.2 m downstream of the tube's exit, when the overpressure reaches its peak at 10.7 ms. The region of the wavefront able to fracture glass (0.15 psig) covers a circular area about 2 m in diameter. A larger tube diameter would increase the diameter of the overpressure above this threshold.

Further analyses were conducted in an attempt to quantify the energy of the source of the blast wave generated upon disc rupture. The commonly used scaled distance concept described in [14] relates the normalised overpressure to the scaled distance normalised with the cube root of the source energy. Consider the overpressure at distance R=4.2 m, where the overpressure for the H_2 case was 4.4 psi and for the CH_4 case was 2.46 psi. Normalising these two overpressures w.r.t. atmospheric pressure and utilising the normalised overpressure vs. scaled distance charts in [14], the resulting scaled distances are 5.3 and 8.6 for pure H_2 and CH_4, respectively. Based on this, the ratio of the blast source energies would be the inverse of the respective scaled distances raised to the power 3. This amounts to a value of 4.272 as shown in Table 2.

We present the argument that the blast energy ought to be proportional to the product of the exit out flow velocity (u) and exit pressure (P), as this represents the energy per unit exit area at the point of rupture over a specific impulse time. If we assume that the impulse time is the same for both H_2 and CH_4 cases, the ratio of the respective $u.P$ is 4.292, which is very close to the ratio of the blast source energies of 4.272. The same calculation procedure was conducted on the overpressures at a distance of 5.0 m. Similar results are obtained as shown in Table 2.

The main conclusion from this comparison is that the blast source energy scaled with the product of $u.P$ can be used to estimate the relative values of the levels of overpressure for future tests involving various blends of NG+H_2. The only two parameters needed for the evaluation are the exit outflow velocity and exit pressure for any specific blend and compare the respective overpressure relative to either the pure H_2 or the CH_4 prediction presented above.

Distance (m)	**4.2**		**5.0**	
	H2	**NG**	**H2**	**NG**
Overpressure (psi)	4.4	2.46	2.8	1.58
Ambient Pressure (psi-a)	13.2	13.2	13.2	13.2
Normalized Overpressure	0.333	0.186	0.212	0.120
Scaled Distance*	5.3	8.6	5.5	9
Ratio of Blast Energies	4.272		4.382	
Exit Velocity, u (m/s)	1083	228	1083	228
Exit Pressure, P (MPa-a)	4.199	4.647	4.199	4.647
Ratio of (u*P)	4.292		4.292	

* Figure 14.59 in [14]

Table 2 Calculation procedure to quantify the blast source energies from a shock tube test.

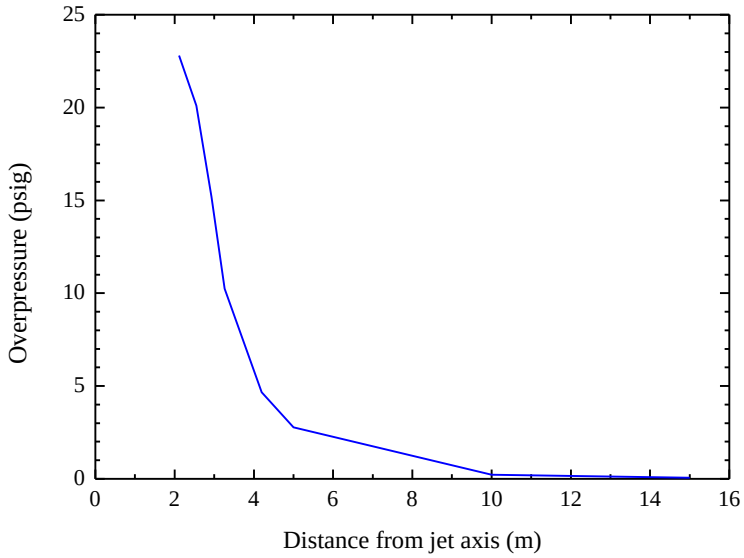

Figure 7: Maximum overpressure along the jet axis

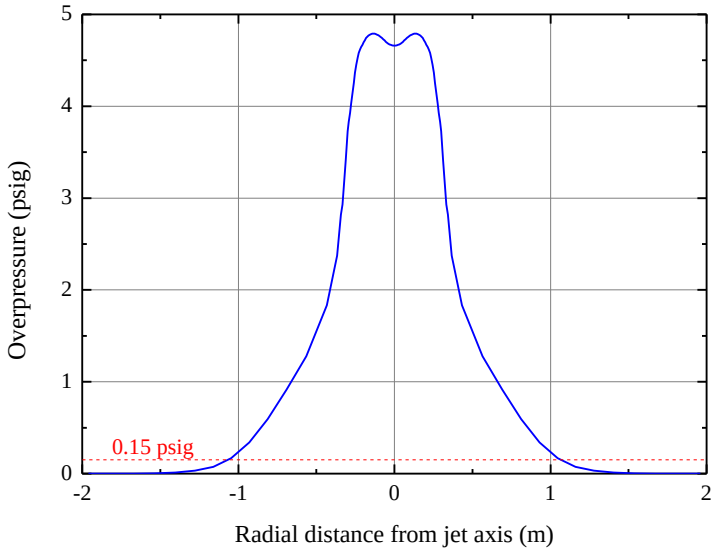

Figure 8: Overpressure profile on the jet cross section at 4.2 m downstream

Figure 9 shows the predicted overpressures produced by CH_4 expansion at different downstream locations. The shock wave produced by CH_4 travels at 359 m/s, which is slightly slower than that of H_2. At 4.2 and 5 m downstream, the evolution of the overpressure behaves differently from that presented by the shock wave produced by H_2. The overpressure initially reaches a small peak, and fluctuates for a relatively long period before reaching the highest peak.

The pressure wave produced by CH_4 expansion appears to be weaker than that produced by H_2. The maximum overpressure values are 2.46, 1.58 and 0.09 psi at 4.2, 5 and 10 m downstream respectively. These are about half the strengths produced by the H_2 expansion. Nonetheless, the shock wave generated by CH_4 can still cause damage to nearby infrastructures. An overpressure of 2.4 psi (4.2 m) is able to shatter non-reinforced concrete or cinder block walls. The reason for not experiencing this in the past during testing with NG is due to the use of barrier concert blocks, the effects of which will be discussed later.

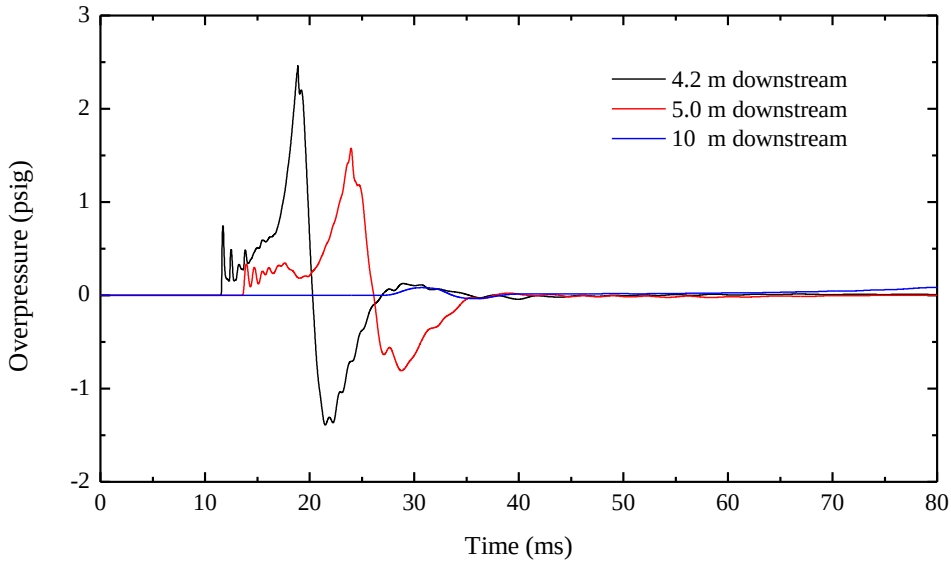

Figure 9: Overpressure histories predicted at different downstream locations (CH_4, 17 MPa)

4.2. Noise Levels

Excessive noise is expected during the release of high-pressure gases. Estimates of noise levels are valuable to develop safety plans and safety measures such as ear protections, exclusion zones and neighbourhood notices.

Noise Exposure Standards define thresholds of noise level and exposure time above which earing damage can occur without hearing protection [16]. Table lists the length of time a person without hearing protection can be exposed for common noise sources and corresponding noise levels [5, 6]. Usually, being near a sound above 115 dB for any length of time without protection can cause permanent hearing damage [6]. At this level, people begin to feel the sound waves in parts of their body.

Sound Pressure Levels (SPLs) at different downstream locations can be estimated based on the overpressure history. The overpressure was recorded every microsecond in the simulations. SPLs were calculated as function of time using a moving window covering a time period of 1 ms. The Root Mean Square (RMS) of the overpressure samples within this window was calculated. Eq. 5 was then used to obtain the SPL within that window.

$$L_p = 20\log_{10}(p_{\mathrm{RMS}}/p_{\mathrm{ref}}) \quad (5)$$

where L_p is the SPL, p_{RMS} is the RMS value of overpressures in the window, and p_{ref} is the reference sound pressure (2×10^{-5} Pa in air).

Noise level (dB)	Sound source	Exposure time
85	Front-end loader	8 hr
100	Sheet-metal workshop	15 min
120	Rock drill	8.8 s
130	Rivet hammer (pain can be felt)	0.9 s
140	Shotgun blast directly beside ear	0.09 s
150	Formula One car at full throttle	N/A
160	Inside jet engine	N/A
170	7,000-HP engine	N/A
180	1 pound of TNT detonating 4.5 m away (15 ft)	N/A

Table 3 Noise levels and the corresponding common noise sources and exposure times [16], [17]

The highest overpressure level in this simulation was recorded downstream, near the jet axis. Figure 10 shows the predicted noise levels produced by H_2 expansion at different downstream locations. The maximum noise level at 5, 10, and 15 m from the jet exit reach 177, 157, and 146 dB respectively. The first incident wave produces the loudest noise, corresponding to the initial overpressure peak shown in Figure 6.

Although the noise level reduces with time after the first overpressure wave passed, fluctuations and slight upward trends are observed at these tree locations. At 5 m, the noise level reduces to about 137 dB at 80 ms. The noise level at 10 m does not vary extensively within the first 80 ms. It just past its last peak at about 75 ms. It is still more than 150 dB at 80 ms, above the level evaluated at 5 m at that instant. Overall, the noise level at 15 m is lower than that at the previous two locations. The initial transient spans the first 20 ms at this location, from 35 to 55 ms approximately. Afterwards, the noise level is fairly stable at about 128 dB; but it exhibits an increasing trend. Permanent hearing damage can be experienced at this distance without protection.

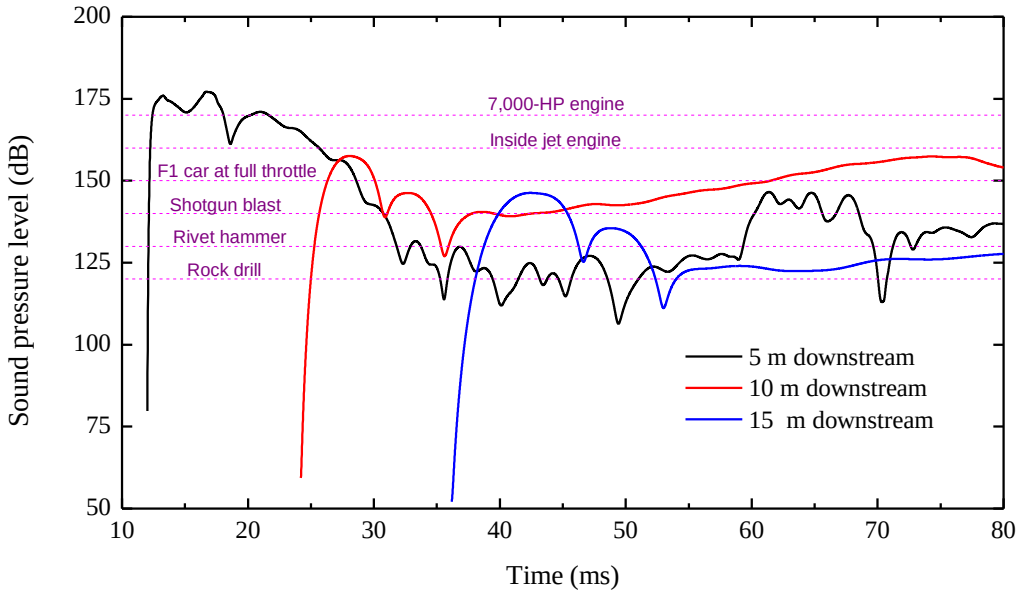

Figure 10: SPL histories predicted at different downstream locations (H_2, 17 MPa)

Figure 11 shows the predicted noise levels produced by CH_4 expansion at different downstream locations. The evolution of noise level with time is similar to that of the H_2 expansion. The highest noise levels are 174, 149, and 140 dB at 5, 10, and 15 m from the jet exit, respectively. At 80 ms, the SPL at 5 m reduces to 115 dB. The SPL at 10 m is reasonably steady at 149 dB at 80 ms. However, the SPL did not reach its final peak within that time frame. The trend is still increasing. The SPL at 15 m is steady from 57 ms after the initiation of the release at about 122 dB.

An increase of 3 dB in SPL yields an increase in loudness[1] of about 25% [18], [19], [20]. The maximum noise level from the expansion of H_2 is higher by 3 to 17 dB relative to CH_4, depending on the location within the first 80 ms of the expansion. There would be a perceived 25% increase in loudness at 5 m distance and about 50% increase in loudness at 10 and 15 m during the H_2 release compared to CH_4.

[1] Despite "loudness" being considered a subjective metric, fair degree of agreement is observed between tested subjects, as discussed in [18].

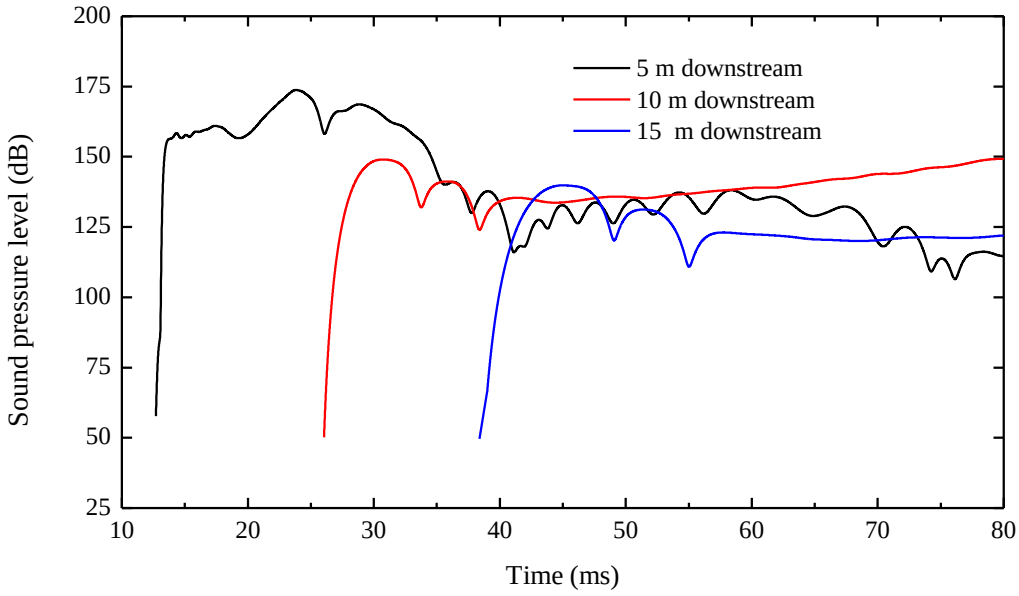

Figure 11: SPL histories predicted at different downstream locations (CH_4, 17 MPa)

4.3. Downstream Flow Temperature

A flammable gas's propension to ignite depends on its minimum ignition energy and its auto-ignition temperature. The former is indicative of the lowest energy required from a point ignition source to ignite the flammable mixture. The latter is indicative of the minimum temperature at which combustion would occur without the presence of an ignition source [21]. Safety considerations surrounding a decompression tube test, or for instance a venting operation of a pipeline section, lead to design out the presence of an ignition source in the vicinity of the expanding jet.

The possibility of auto-ignition is less obvious. The auto-ignition temperature of a mixture is not a constant. It depends on the concentration of the fuel, the pressure as well as other factors such as the characteristics of the flow, and for ignition within a containment vessel, the geometry of the vessel itself [21], [22]. The auto-ignition temperature typically decreases with an increase in pressure. Decompression tube tests of lean and rich natural gas mixtures and 'routine' venting operations of the past many decades demonstrate auto-ignition of methane is not of practical concern. In contrast, the combustion observed during the first decompression test of pure H_2 may have been the result of an auto-ignition. The CFD simulations carried out provide some insight on the matter.

The temperature in the near field was monitored in the simulations. Figure 12 and Figure 13 show the temperature contours near the jet exit for H_2 and CH_4 respectively. Three instants are shown for each simulation: 0.1, 0.5 and 1 ms. The expanding gas compresses the atmosphere almost instantly. high temperature region develops almost immediately at the interface between the test mixture and the ambient air, as shown at 0.1 ms. Adiabatic heating takes place within a thin crown enveloping the test mixture.

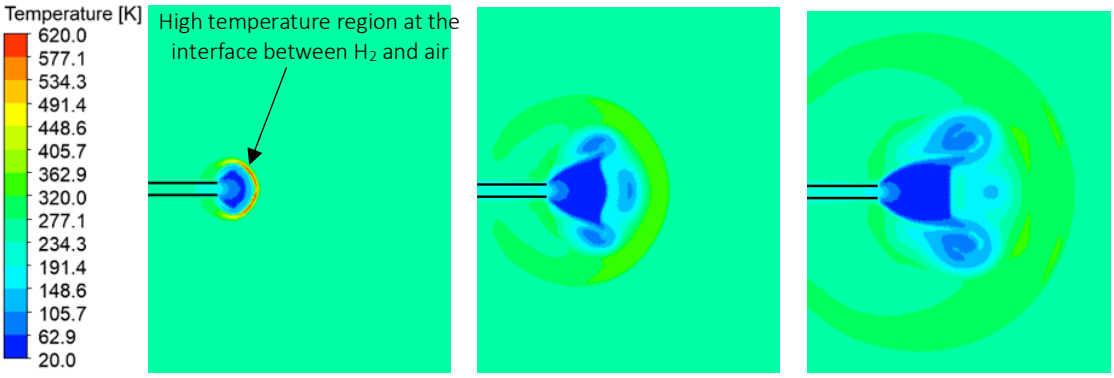

a. 0.1 ms b. 0.5 ms c. 1 ms

Figure 12: Temperature contours near the jet exit (H_2, 17 MPa).

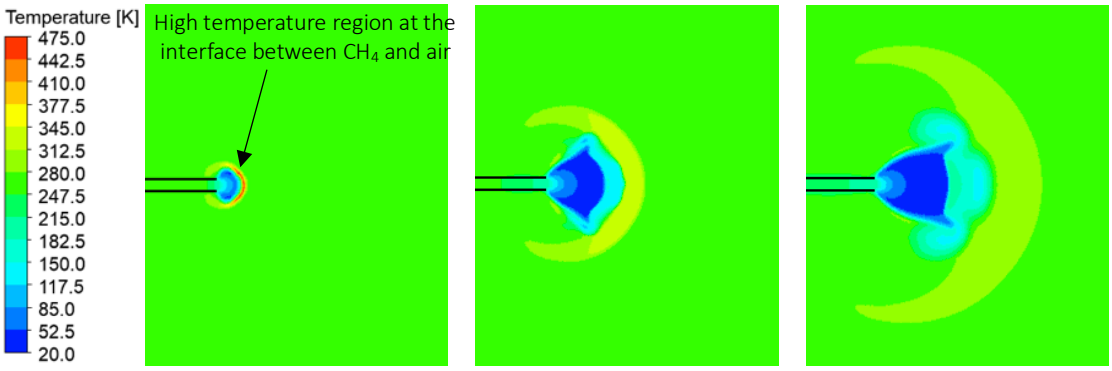

a. 0.1 ms b. 0.5 ms c. 1 ms

Figure 13: Temperature contours near the jet exit (CH_4, 17 MPa).

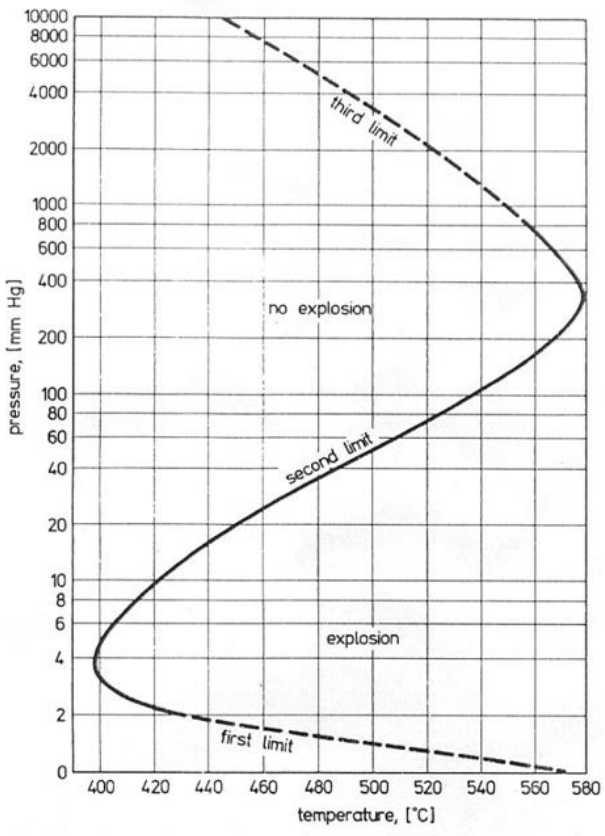

Figure 14: Pressure-Temperature limit of a stochiometric hydrogen-oxygen mixture [23].

The maximum temperature observed from the H_2 release (620 K, or 347 °C) at 0.1 ms is higher than that observed from the CH_4 release (475 K, or 202 °C). However, it also decreases at a faster rate than that from the CH_4 release. The development of the crown occurs at the interface between the gas in the decompression tube and the atmosphere. It is the region where the two begin to mix. A gradient of H_2-O_2 concentration progressively develops across that interface; stochiometric condition exists somewhere within that gradient.

Figure 14 shows the pressure-temperature plot for auto-ignition of a stochiometric H_2-O_2 mixture, called the self-ignition peninsula from Lewis and von Elbe [23]. The plot is relevant to a contained ignition in a 74 mm diameter vessel. The conditions are different from that surrounding the expanding jet considered here. Nevertheless, the plot is valuable to draw general conclusions, especially in view of the scarcity of similar data in the literature. Conditions above atmospheric pressure, above 685 mm Hg in Didsbury, are along the third limit as shown in Figure 14. This branch of the plot is an extrapolation. It shows a decrease in ignition temperature with an increase in pressure.

The upper end of the plot shows the auto-ignition temperature of H_2-O_2 at 10,000 mm Hg (1.33 MPa) and 445 °C. The high temperature crown in Figure 12 is about 100 °C lower. The local pressure from the simulation was also lower than 1.33 MPa at this point. Accordingly, auto-ignition appears unlikely to occur after the first 0.1 ms of the expansion. It is worth investigating the state of the crown at earlier instants.

The temperature field along the jet axis indicates that the highest temperature occurs approximately 4 cm and 5 cm downstream for the H_2 and CH_4 release respectively. Figure 15 shows the temperature histories monitored at these two locations. The shock at the H_2-air interface produces the highest temperature at 1100 K (827 °C) at 2.5×10^{-5} s. This is largely above the auto ignition temperature expected even at atmospheric pressure, see Figure 14. In comparison, the highest temperature from the CH_4 release is less than half that of H_2, at 558 K and 5×10^{-5} s.

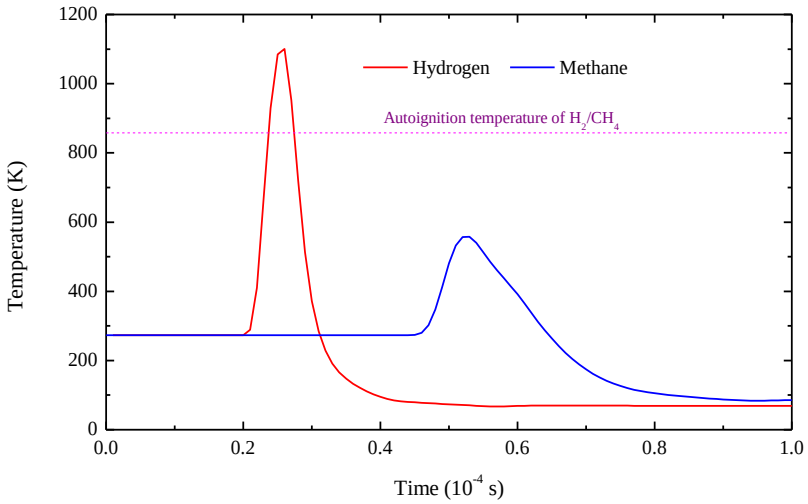

Figure 15: Temperatures monitored near the jet exit for H_2 and CH_4 releases

Figure 16 shows the H_2 concentration and the pressure at 4 cm downstream along the jet axis. The red part of the curves marks the region where the temperature is above the auto-ignition temperature at atmospheric pressure. The H_2 fraction and pressure increase in this region. A large part of the H_2 fraction curve lies within the flammable region of H_2 between 4% and 75%. The pressure at this location is above the ambient pressure, between 0.4 and 1.5 MPa, or between 3,000 and 11,250 mm Hg.

According to Figure 14, any temperature above 773 K (500 °C) would lead to auto-ignition at a pressure above 0.4 MPa. The rise in temperature and pressure, combined with the evolution of H_2 fraction within

the crown would rapidly bring the three conditions necessary to cause ignition of H_2 [23]. Ignition would be expected to occur sometime between $2.5e^{-5}$ and $3e^{-5}$ s according to the simulation. In [24], the authors state that the flame initiated by a H_2 jet could be brought to the boundary layer by the vortex. In such case the flame is likely to develop stably and a stable combustion zone would form.

The present simulation did not attempt to reproduce the combustion mechanism. The combustion would increase the temperature field, lead to a supplementary release of energy and affect the flow. The process would in turn affect the overpressure wave and the noise levels discussed in the previous sections.

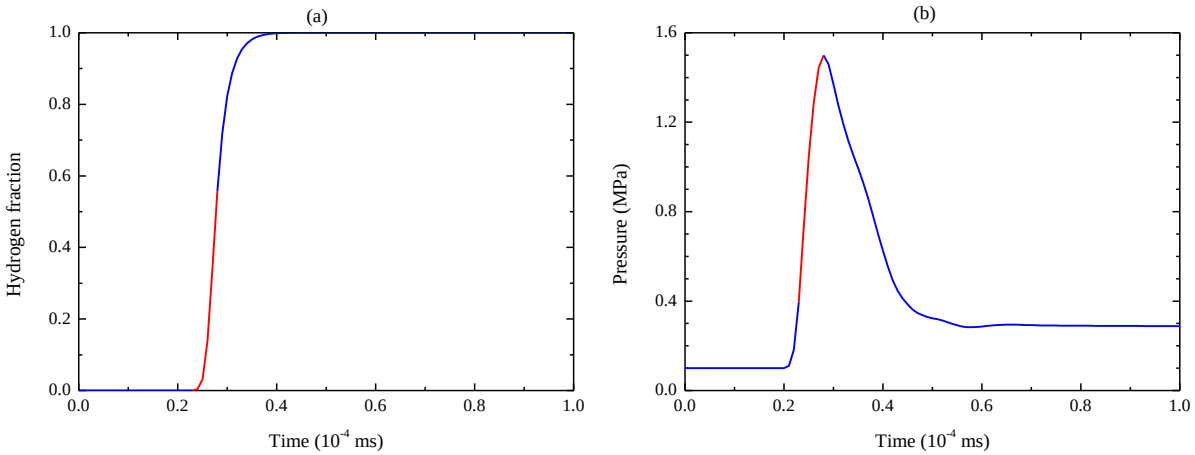

Figure 16: H_2 fraction and pressure monitored at 4 cm downstream for H_2 releases

5. RISK MITIGATION

Over 150 tests were conducted over the years at TC Energy's Gas Dynamics Test Facility. Significant expertise has been developed as a result. Shock waves and damaging outflows are expected to occur during decompression tests. Concrete blocks are placed between the shock tube exit and the downstream building to avoid damage.

Figure 17 shows the L-shape arrangement of the concrete blocks protecting the building. The tube faces the east end of the building, at its southern limit. A series of blocks face the shock tube. A second series of blocks is placed north of the first series to limit the propagation of the overpressure wave and flow in the north-west direction.

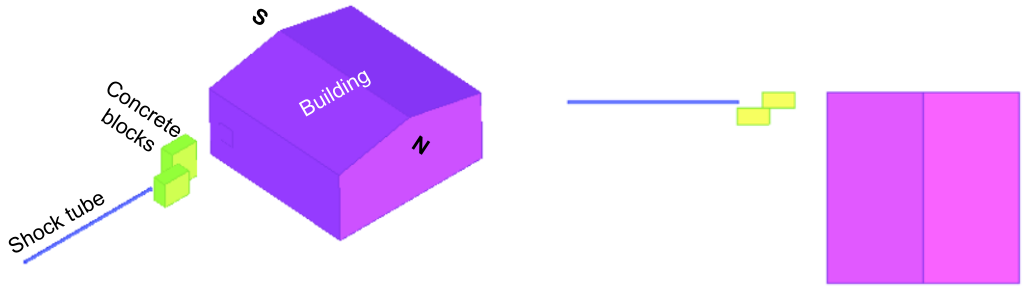

(a) 3-d view (b) top view

Figure 17: Main components in the TCE test site

A 2-dimensional axisymmetric CFD model was used to evaluate the effect of concrete blocks for risk mitigation purposes. A 3-dimensional model is also planned as part of this work. The axisymmetric model limits the use of objects with circular cross-sections. It is a departure from reality. Two cases are shown schematically in Figure 18.. Case 1 uses one concrete block facing the shock tube exit, with no

lateral obstruction. This is to account for the effect of the shock wave bypassing the concrete block on the south side, see Figure 17. Case 2 impedes the jet flow in all lateral directions. Dimensions used in these two cases were determined according to those used in the experiment. In Case 1, the radius of the concrete block is equal to the distance between the shock tube axis and the south wall of the concrete block. In Case 2, dimensions reflect the experiment somewhat more closely with three rows of concrete blocks.

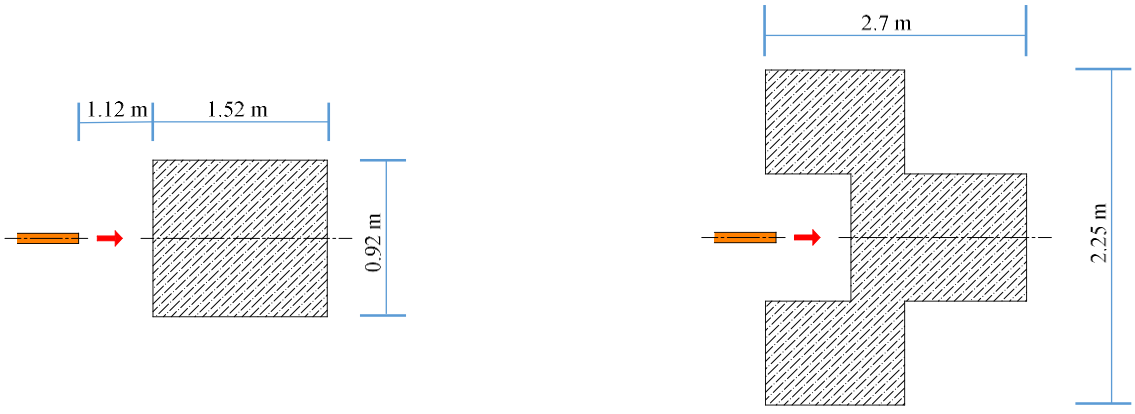

a. Case 1 b. Case 2

Figure 18: Schematic of cases simulated with concrete blocks (not to scale)

Figure 19 shows the time histories for the overpressure field predicted on the wall surface of the building for Case 1 and 2. The concrete blocks significantly reduce the overpressure strength. In Case 1 (Figure 19.a), the strength of the shock wave can be reduced to one third and one fourth of its original value for H_2 and CH_4 respectively. The overpressures due to the H_2 release can still cause 'partial demolition to house structures'. 'Limited minor structural damage' would be caused by the CH_4 release. The arrival of the first peak of overpressures on the building wall is delayed by about 1 ms for both release.

Case 2 is shown in Figure 19b. The strength of the waves on the building wall is significantly reduced compared to that of Case 1. The maximum H_2 release's overpressure reduces to less than one tenth of that observed in Case 1. This is insufficient to cause glass failure. The strength of the maximum overpressure for the CH_4 release is again about half that of the H_2 release. The arrival of the peak pressure on the building wall is delayed by about 10 ms with this configuration of blocks. This is because the waves are initially reflected back upstream by the blocks before finding their way towards the building.

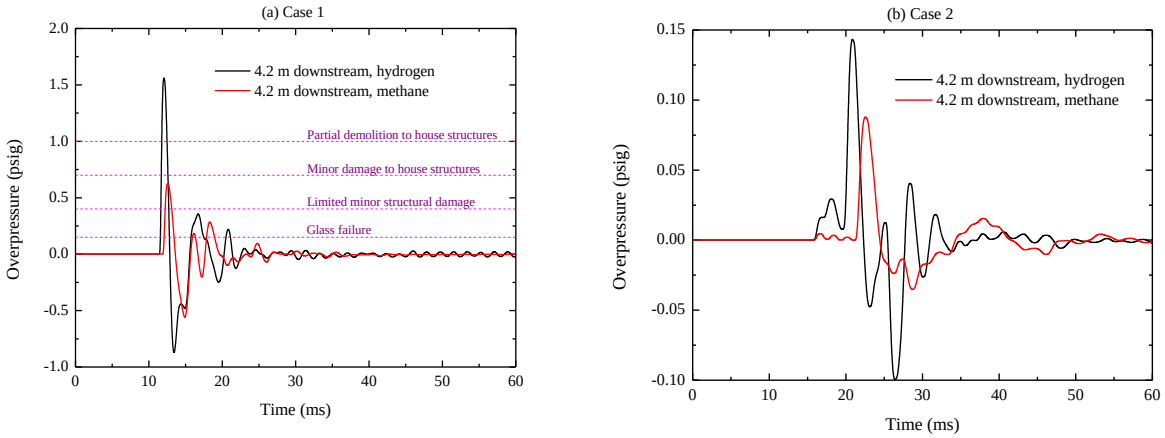

Figure 19: Overpressure histories predicted on the building wall: H_2 vs CH_4

Figure 20 shows the time histories for the noise levels predicted at 10 and 15 m from the shock tube exit for Case 1 and Case 2. The loudest noise is heard in the downstream direction in Case 1. It is heard in the upstream direction in Case 2. In Case 1, and compared to the case without building blocks (section 4.2), the highest noise levels from the H_2 release at 10 and 15 m can be reduced by 8 dB and 2 dB respectively. The highest noise levels at 10 and 15 m are reduced by 6 dB and 1 dB, respectively, for the CH_4 release. The building block contributes to a faster decay of the noise level. At 80 ms, the SPLs from the H_2 release at 10 and 15 m reduce to 85 and 107 dB respectively. Similar reductions can be seen in the CH_4 release. The noise from the H_2 release is still about 6 dB louder than that from the CH_4 release.

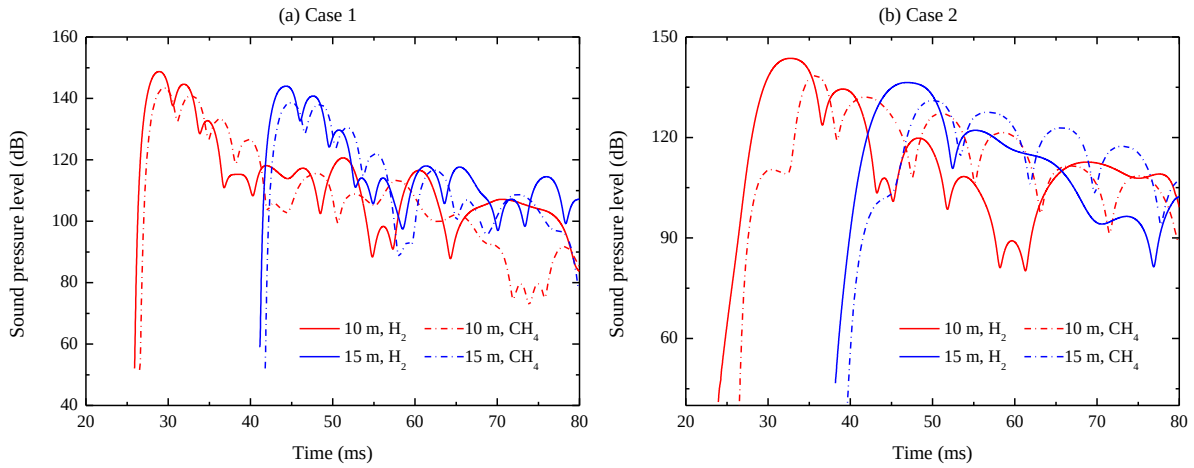

Figure 20: SPL histories predicted for Case 1 and Case 2: H_2 vs CH_4

In Case 2 (Figure 20b), the highest noise levels at 10 and 15 m from the H_2 release are 143 and 136 dB respectively. This is 6 and 8 dB lower than observed in Case 1. Similar reduction is predicted for the CH_4 release. Compared to Case 1, the SPL reduces more slowly in Case 2. However, the SPLs at 10 and 15 m are all below 110 dB for both releases at 80 ms.

The concrete blocks are not able to prevent the development of the initial high temperature crown discussed in the previous section. Further, objects present in the H_2 stream can promote the chance of ignition [22] [25]. However, the configuration of Case 2 will mostly redirect the released hydrogen towards the upstream direction (see Figure 21). If ignition does occur, then the overpressure wave due to ignition would also be reflected by the concrete blocks. This configuration would limit damage to the downstream building. A more realistic three-dimensional configuration with a U-shape series of blocks and the ground surface would be expected to redirect the flow as well as the overpressure waves in the upstream and upward directions.

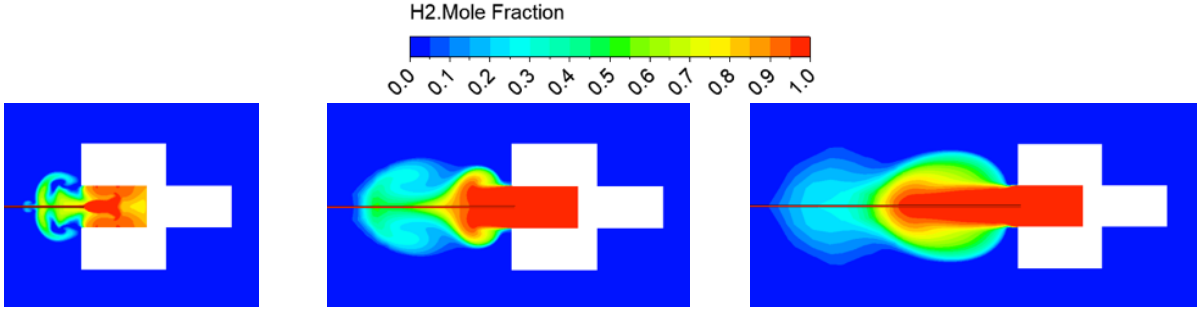

(a) 10 ms (b) 30 ms (c) 60 ms

Figure 21: H_2 concentration contours predicted in Case 2

In [26], Lowesmith and Hankinson found that the overpressures due to a NG pipeline rupture are about twice those produced by the ignition of the gas. Assuming that the ignition of the H_2-O_2 mixture would

produce an overpressure equivalent to half that of the H_2 release, then temperature and overpressures associated to ignition may need to be considered in more details in the future.

Overall, downstream concrete blocks can effectively reduce the risks of overpressure and noise, and prevent the released H_2 from spreading downstream, especially when the lateral travelling of the jet flow is impeded like in Case 2.

6. CONCLUSIONS

A shock tube test for the decompression of pure H_2 was conducted at TC Energy's Gas Dynamics Test Facility in Didsbury, Canada, under the supervision of NOVA Chemical. The decompression wave speed was successfully measured. Good agreement between model and experiment was observed at high decompression wave speed velocities. Questions remain on the impact of frictional effects at the tail of the decompression curve.

High noise level, exceeding that from tests conducted with natural gas or CO_2 mixtures, as well as ignition of the outflow was witnessed during the test. To better understand risks from overpressure wave, noise levels and ignition associated with H_2 decompression and atmospheric expansion, CFD models were developed to replicate the environment of the test program conducted at the TCE site. The simulations were carried out to compare H_2 and CH_4 releases at 17 MPa.

Results show that the strength of overpressures generated by a H_2 release can reach two times that of a CH_4 release. Without mitigations, damage may be caused to nearby building with both H_2 and CH_4 releases. However, the damage due to a H_2 release will be more severe.

A method to estimate the blast source energy from a shock tube test is proposed which was found to be scaled with the product of $u.P$. This value can be used to estimate the relative levels of overpressure for any tests involving blends of NG+H_2. The only two parameters needed for the evaluation are the exit outflow velocity and exit pressure for any specific blend and compare the respective overpressure relative to either the pure H_2 or the CH_4 prediction presented in this paper.

A decompression tube test produces a loud noise. A H_2 release is about 6 dB higher than a CH_4 release, subjectively this is about 50% louder.

High temperatures above the auto-ignition temperature are generated in a H_2 release. It is highly possible that auto-ignition would take place within the first instants of the release.

A feasible way to mitigate risks in the decompression tests is to place concrete blocks between the shock tube exit and the downstream facilities. The jet flow propagation should be impeded in both the downstream and lateral directions. CFD simulations show that overpressures and noises can be effectively reduced. The H_2 outflow can be reflected back upstream or upward, limiting direct exposure of potential downstream facilities to the likely combustion of H_2.

7. ACKNOWEDGEMENT

Future Fuels CRC is supported through the Australian Government's Cooperative Research Centres Program.

The shock tube facility is part of a high-pressure natural gas test facility located in Didsbury, Alberta, Canada and is owned by TC Energy. Permission to use the shock tube and associated auxiliary system, unique instrumentation features and accurate data acquisition and processing schemes are greatly appreciated.

8. REFERENCES

[1] IPCC, Global Warming of 1.5 degC, "An IPCC special report on the impacts of global warming of 1.5 degC above pre-industrial levels and related global greenhouse gas emission pathways (...)," in *IPCC Working Group I*, Saint-Aubin, France, 2018.

[2] International Energy Agency (IEA), "The future of hydrogen: Seizing today's opportunities," IEA, Paris, France, 2019.

[3] W. A. Maxey, "Fracture Initiation, Propagation and Arrest," in *5th Symposium on Line Pipe Research*, Houston, Texas, 1974.

[4] W. A. Maxey, "Gas expansion studies," AGA NG-18 report 133, 1983.

[5] K. K. Botros, J. Geerligs and R. J. Eiber, "Measurement of decompression wave speed in rich gas mixtures at high pressures (370 bars) using a specialized rupture tube," *Journal of Pressure Vessel Technology,* vol. 132, pp. 051303-1, 2010.

[6] K. K. Botros , "Measurements of speed of sound in lean and rich natural gas mixtures up to 37 MPa using a specialized rupture tube," *Int. J. Thermophys.,* vol. 31, no. 11, pp. 2086-2102, 2010.

[7] K. K. Botros, J. Geerligs, B. Rothwell and T. Robinson, "Measurements of decompression wave speed in binary mixtures of carbon dioxide mixtures and impurities," *Journal of Pressure Vessel Technologies,* vol. 139, no. 2, pp. PVT-15-1107, 2017.

[8] K. K. Botros, S. Igi and J. Kondo, "Measurement of decompression wave speed in natural Gas containing 2-8% (Mole) Hydrogen by a specialized shock tube," in *11th International Pipeline Conference IPC2016, 26-30 September 2016*, Calgary, Canada, 2016.

[9] S. Igi, "Running ductile fracture analysis using experimental crack-velocity curve - a case study," vol. 4th Quarter, pp. 257-265, 2016.

[10] G. Michal and C. Lu, "Development of a pipeline fracture control software – Phase III, Final Report project RP3-02I," Energy Pipelines CRC, 2013.

[11] W. Wagner, "GERG 2008 user manual - Description of the Software Package for the calculation of thermodynamic properties from the GERG-2004 XT08 wide-range equation of state for natural gases and other mixtures," Ruhr-Universitat Bochum, Bochum, Germany, 2009.

[12] K. K. Botros, B. Rothwell, C. Buterbaugh, C. Hsiao, P. Venton and R. Cooper, "Measurement od decompression wave speed in mixtures of CO2 and impurities and comparison with predictions by different EOS," in *18th Biennial Joint Technical Meeting 2011 (JTM2011)*, San Francisco, California, USA, May 2011.

[13] C. Lu, G. Michal, A. Elshaomi, A. Godbole, P. Venton, K. K. Botros, L. Fletcher and B. Rothwell, "Investigation of the effects of pipe wall roughness and pipe diameter on the decompression wave speed in natural gas pipelines," in *9th International Pipeline Conference IPC2012, 24-28 September 2012*, Calgary, Alberta, Canada, 2012.

[14] D. Y. Peng and D. B. Robinson, "A new two-constant equation of state," *Ind. Eng. Chem/ Fundam.,* vol. 15, no. 1, pp. 59-64, 1976.

[15] F. P. Lees, Loss prevention in the process industries, vol. 1, Londan & Boston: Butterworth-Heinemann, 1980, p. ISBN 0408106042.

[16] Safe Work Australia, "Managing noise and preventing hearing loss at work: code of practice," Safe Work Australia, Canberra, ACT, Australia, 2015.

[17] P. Ortiz, "Decibel equivalent tab;es: What does each volume sound like?," 2022. [Online]. Available: https://housegrail.com/decibel-equivalent-table-whats-how-loud. [Accessed 28 April 2022].

[18] R. M. Warren, "Quantification of Loudness," *JSTOR & University of Illinois Press,* vol. 86, no. 4, pp. 807-825, 1973.

[19] R. M. Warren, "Elimination of biases in loudness judgments for tones," *The Journal of the Acoustical Society of America,* vol. 48, pp. 1397-1403, 1970.

[20] T. D. Rossing, F. R. Moore and P. A. Wheeler, The Science of Sound, Chapter 6: Sound Pressure, Power, and Loudness, Pearson Education, 2002.

[21] M. Caron, M. Goethals, G. De Smedt, J. Berghmans, S. Vliegen, E. Van't Oost and A. van den Aarssen, "Pressure dependence of the auto-ignition temperature of methane / air mixtures," *Journal of Hazardous Materials,* vol. A65, pp. 233-244, 1999.

[22] A. G. Venetsanos, P. Benard, E. Papanikolaou, K. Verfonden, E. Gallego, J. M. Martin-Valdepenaz and M. A. Jimenez, "Biennial report on hydrogen safety. Chapter III: Accidental phenomena and consequences," HySafe, June 2007.

[23] B. Lewis and G. von Elbe, Combustion, flames and explosions of gases, vol. 3rd Edition, New York: Academic Press, 1987.

[24] X. Pan, W. Yan, Y. Jiang, Z. Wang, M. Hua, Q. Wang and J. Jiang, "Experimental investigation of teh self-ignition and jet flame of hydrogen jets released under different conditions," *ACS Omega,* vol. 4, no. 7, pp. 12004-12011, 2019.

[25] F. L. Dryer, M. Chaos, Z. Zhao, J. N. Stein, J. Y. Alpert and C. J. Homer, "Spontaneous ignition of pressurized releases of hydrogen and natural gas into air," *Combustion Science and Technologies,* vol. 179, pp. 663-694, 2007.

[26] B. J. Lowesmith and G. Hankinson, "Large scale experiments to study fires following the rupture of high pressure pipelines conveying natural gas and natural gas/hydrogen mixtures," *Process Safety and Environmental Protection,* vol. 91, no. 1, pp. 101-111, 2013.